Jurnal Polimesin
Department of Mechanical Engineering
State Polytechnic of Lhokseumawe
http://e-jurnal.pnl.ac.id/polimesin
e-ISSN : 2549-1999 No. : 3 Month : June
p-ISSN : 1693-5462 Volume : 23 Year : 2025

Processing Dates: Received on 2024-07-30, Reviewed 2024-11-17, Accepted on 2025-06-27 and Available online on 2025-06-30

Design optimisation of a shell-and-tube heat exchanger for cold energy recovery in LNG regasification

Haiqal Irfansyah, Sarwo Edhy Sofyan*, Razali Thaib, Akram Tamlicha

Department of Mechanical Engineering, University of Syiah Kuala, Banda Aceh, 23111, Indonesia
*Corresponding author: sarwo.edhy@usk.ac.id

Abstract

The efficient utilisation of energy resources is a key concern in industrial operations, particularly within the liquefied natural gas (LNG) sector. During the regasification process, substantial amounts of cold energy are released as LNG transitions from its liquid to gaseous state. This cold energy, often wasted by being discharged into the environment, presents an opportunity for recovery and use in various applications such as cold storage and data centre cooling. While the utilisation of LNG cold energy has been widely explored for specific applications, including data centre cooling, electricity generation, and cryogenic systems, existing studies typically focus on individual technologies rather than a comprehensive optimisation of heat exchanger design for cold energy recovery. Therefore, there remains a significant gap in optimising heat exchanger configurations that maximise cold energy extraction while enabling broader industrial integration. This study addresses that gap by optimising the design of a shell-and-tube heat exchanger to recover cold energy from the LNG regasification process at PT Perta Arun Gas, based on an LNG flow rate of 30 million standard cubic feet per day (MMSCFD). The design optimisation was performed using Aspen Exchanger Design and Rating (Aspen EDR) software. Propane was selected as the secondary fluid for extracting cold energy from LNG due to its exceptionally low-temperature performance (freezing point: -188°C) and proven safety in food-related environments. The shell-and-tube heat exchanger design was optimised by the standards and configurations defined by the TEMA designation. The resulting optimal configuration comprises a shell-and-tube heat exchanger with a tube diameter of 13 mm, a tube length of 2,550 mm, a shell diameter of 162.74 mm, a baffle pitch of 135 mm, 16 baffles, a single tube pass, and 54 tubes. This design achieves a heat transfer rate of 478.5 kW, with an estimated cost of USD 23,895.

Keywords:
Shell and tube heat exchanger, LNG, design optimisation, cold energy, energy recovery

1 Introduction

PT Perta Arun Gas is a company engaged in the regasification of liquefied natural gas (LNG), LNG Hub, and several other supporting businesses. Currently, PT Perta Arun Gas is the only company with regasification facilities in the Aceh and North Sumatra regions. Its strategic geographical location, supported by sea transportation routes and adequate dock facilities, facilitates easy loading and unloading processes, positioning the company as a key player in the region's LNG infrastructure.

Central to the operations of PT Perta Arun Gas is the regasification process, a crucial step in the LNG value chain that enables the delivery of natural gas to end users in its gaseous state. After LNG is transported as a cryogenic liquid at approximately -160°C, it must be converted back into its gaseous form at receiving terminals. This is achieved through regasification systems that use heat exchangers to transfer thermal energy, typically from seawater or glycol-water solutions, to the LNG. As the LNG absorbs heat, it vaporises and transitions into a gaseous state, ready for distribution to local pipelines. Advanced regasification technologies, such as open-rack vaporisers (ORVs) and submerged combustion vaporisers (SCVs) [1][2][3][4], ensure efficient and reliable processing, enabling PT Perta Arun Gas to meet growing energy demands.

Currently, a significant portion of the cold energy generated during the LNG regasification process is wasted into the environment. As LNG is converted from its cryogenic liquid form back into gas, heat must be transferred to the LNG through a regasification system, typically involving heat exchangers that use seawater [5]. However, the process is not entirely efficient, and a large amount of cold energy is dissipated into the surrounding environment. This waste occurs because the cooling medium, such as seawater, is not fully optimised for energy recovery. The release of this cold energy into water bodies contributes to energy inefficiencies, reducing the overall sustainability of LNG regasification. While the primary goal of regasification is to vaporise LNG for distribution, the unused cold energy could serve as a valuable resource for other applications [6]. However, without adequate systems in place to capture and utilise this cold energy, it remains a largely untapped resource that could otherwise be harnessed for industrial or cooling purposes[7][8][9][10]. Therefore, addressing this waste and developing technologies to recover and reuse this cold energy is crucial for improving the energy efficiency and environmental sustainability of LNG infrastructure.

Recent research has focused on the recovery of wasted cold energy from the LNG regasification process for various cooling energy applications, such as cold storage [11][12] and data centre cooling [13]. Studies have shown that the cold energy released during regasification, typically dissipated into the environment, can be captured and redirected to enhance the efficiency of cooling systems. For instance, one study explored the potential of using recovered cryogenic cold energy to power air-blast freezers in cold storage facilities [14], reducing the need for conventional refrigeration methods that rely on electricity. Similarly, in data centres, where cooling demands are high due to the heat generated by servers, the use of LNG-derived cold energy can significantly lower operational costs and energy consumption. By utilising this otherwise wasted cold energy, these industries can achieve a more sustainable cooling solution, improving both environmental impact and energy efficiency. The successful implementation of such technologies would not only optimise the LNG regasification process but also contribute to broader efforts to recover and repurpose energy in industries with high cooling requirements. This approach presents a promising avenue for reducing energy waste and supporting the transition toward greener, more efficient industrial practices [15].

Numerous studies have addressed the recovery of waste cold energy from LNG regasification. Yadav et al. [16] investigated utilising cold energy from the LNG regasification process for data centre cooling and electricity generation. Zheng et al. [17] presented a multi-objective optimisation and performance study for a system that combines refrigeration, power production, air separation, and ice thermal storage based on LNG cold energy utilisation. Cai et al. [18] presented exergy and economic evaluation of LNG cold energy power generation systems employing various cold energy application techniques. Wang et al. [19] analysed the cold energy use in cryogenic dual-energy heavy-duty trucks integrated with LH2/LNG-cooled shielding systems. Franco and Giovannini [20] presented an ideal configuration of direct expansion systems for

generating electricity through the recovery of cold energy from LNG. Wu et al. [21] proposed a comprehensive approach to recovering LNG cold energy for balancing supply and demand by utilising energy storage systems.

While the utilisation of cold energy from the LNG regasification process has been extensively studied, significant gaps remain in optimising its recovery and application. Existing research has demonstrated the feasibility of using LNG cold energy for data centre cooling, electricity generation, and various integrated systems, optimising its use for refrigeration, power generation, air separation, and ice thermal storage. Studies have also assessed the exergy and economic performance of different cold energy utilisation techniques and explored its applications in cryogenic heavy-duty trucks. Additionally, proposed configurations for direct expansion systems highlight the potential for generating electricity from LNG cold energy. These studies often focus on specific applications or technologies without addressing the holistic optimisation of heat exchanger design for cold energy extraction in LNG regasification.

Therefore, there is a pressing need to bridge this gap by developing and optimising heat exchanger designs that not only enhance cold energy recovery but also support diverse industrial applications. Addressing this gap will contribute to improving the energy efficiency and sustainability of LNG infrastructure while expanding its potential for industrial integration.

This study aims to identify the best design for the extraction process and create a heat exchanger that can extract cold energy from the LNG regasification process at PT Perta Arun Gas at a flow rate of 30 MMSCFD.

2 Methods

2.1 Data Collection

Data collection was conducted at PT Perta Arun Gas and includes a process flow diagram of the LNG regasification system, along with specifications such as the composition and physical properties of LNG. This information serves as input for the design and optimisation of the heat exchanger using relevant software tools. A simplified schematic of the regasification process, presented in Fig. 1, provides a visual aid to support the research.

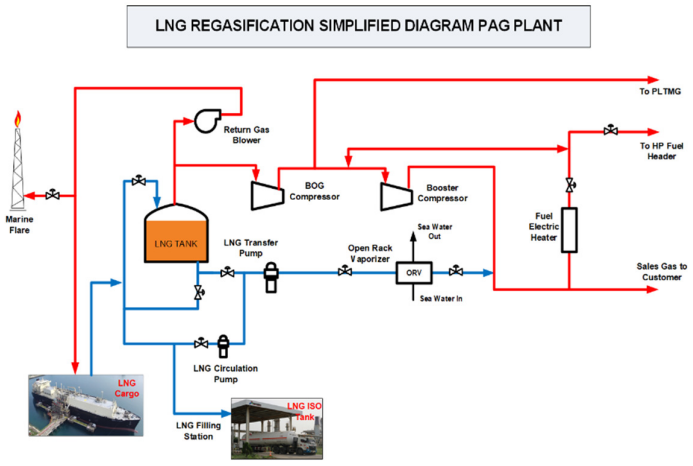

Fig. 1. LNG regasification process flow diagram [1]

Fig. 1 outlines the LNG regasification workflow at PT Perta Arun Gas. The process initiates with transferring LNG from cargo ships to onshore storage tanks using dedicated pumps. From storage, LNG is pumped through circulation systems to the ORV, where seawater facilitates heat exchange to convert LNG into natural gas. The regasified natural gas proceeds through booster compressors and the Boil-Off Gas (BOG) compressor system, which stabilises pressure and mitigates energy losses by managing vaporised gas. Depending on operational demands, a fraction of the gas is diverted to fuel gas heaters or high-pressure fuel headers. Additionally, a return gas blower ensures flow stability and pressure equilibrium. This schematic highlights the primary process stages and essential equipment, offering a structured basis for subsequent thermodynamic evaluations and heat exchanger optimisation in this research.

2.2 LNG Composition

The composition of the compounds contained in LNG used in this study is presented in Table 1.

Table.1 LNG composition [1].

Component	Mole fraction
N2	0.099
CH4	95.713
C2H6	3.254
C3H8	0.667
i C4H10	0.124
n C4H10	0.148
i C5H12	0.015
TOTAL	100.000

2.3 LNG Flow Specifications

The specification data for LNG used in this study is summarised in Table 2. Based on Table 2, the LNG specifications at the discharge pump operating at a pressure of 56 kg/cm² include a temperature of -156 °C and a flow rate of 100 MMSCFD. These parameters are used as input for simulation processes in Aspen HYSYS and Aspen Exchanger Design and Rating (EDR) software

Table.2 LNG flow specification [1].

Stream Name	Liquefied Natural Gas
Vapour/Phase Fraction	Cair
Temperature [°C]	-156
Flow Rate [MMSCFD]	100
Pressure [kg/cm^2]	56

2.4 Coolant Selection

Propane was selected as the coolant because of its outstanding low-temperature performance (freezing point: -188°C) and its safety in food-related applications. It does not present any risks of freezing or icing and is non-toxic, which makes it appropriate for food processing.

Table.3 Coolant Selection Criteria [2].

Substance	Food Poisoning (Yes/No)	Freeze Point (°C)	Freezing Potential	Flammable
Propane	Yes	-188	No	Yes
Ethylene- Glycol	Yes	-12.9	Yes	No
Propylene	Yes	-185.2	No	Yes
Butane	Yes	-140	No	Yes
Iso Butane	Yes	-159.42	No	Yes
DME	Yes	-45.5	Yes	Yes
Ammonia	Yes	-77.7	Yes	Yes

2.5 Heat Exchanger Selection

The shell-and-tube heat exchanger is selected for its ability to operate under high pressures (up to 55.2 MPa), elevated temperatures (up to 538 °C), and large heat transfer areas (up to 2,787 m² per shell). It is capable of handling a diverse array of fluids, including gases, thick liquids, and substances undergoing phase changes, while facilitating multi-stream exchanges. Although it is typically less compact and more challenging to service, its robustness, minimal leakage potential, and ability to resist fouling and corrosion make it a dependable and adaptable choice for demanding thermal applications.

2.6 *TEMA* designation

Table.4 TEMA designation of heat exchanger

Category	Item	Remarks
TEMA type	Front Head Type	B
	Shell Type	E
	Rear Head Type	M
Tubes	Diameter	13 mm; 16 mm; 19.05 mm; 20 mm; 25 mm; 25.4 mm; 30 mm; 38 mm
	Pattern	30-Triangular
Baffles	Type	Single Segmental
	Orientation	Horizontal
Material	Shell & Tubes	Stainless Steel 304

Table 4 shows the TEMA designation used as an input parameter in the heat exchanger design within the Aspen EDR software. Aspen EDR was selected for the heat exchanger design and optimisation in this study due to its robust capabilities in both rating and sizing tasks, as well as its support for a wide range of heat exchanger configurations compliant with TEMA standards.

2.7 Heat Exchanger Design Limitations

The design optimisation of the heat exchanger in this study is subject to the following constraints:

1. The heat exchanger is designed to extract cold energy from LNG at a flow rate of 30 MMSCFD
2. The temperature change of LNG during the cold energy extraction process is limited to 20°C to ensure the LNG remains in the liquid phase and can be returned to the ORV inlet. ($\Delta T\_LNG = 20°C$).
3. The coolant used in the cold energy extraction process is propane, which is planned to enter the heat exchanger at -26°C and exit at -100°C. (T_i Propane = -26°C, T_o Propane = -100°C).
4. The heat transfer capacity specified for a flow rate of 30 MMSCFD is 478.5 kW.
5. Tube diameter sizes are selected based on TEMA standards: 13 mm, 16 mm, 19.05 mm, 20 mm, 25 mm, 25.4 mm, 30 mm, and 38 mm.

2.8 Heat Exchanger Design Input Data

Table 5 presents the heat exchanger process data, which serve as input parameters for the software during the design process.

Table. 5 Heat exchanger process data

Parameter	Propane (Hot Stream)	LNG (Cold Stream)
Mass Flow Rate (kg/h)		25130
Inlet Temperature (°C)	- 26	- 156
Outlet Temperature (°C)	- 100	- 136
Vapor Fraction	Liquid	Liquid
Pressure (kg/cm^2)	2.14	56
Allowable Pressure Drop (kg/cm^2)	0.20	0.20
Fouling Resistance (m^2K/W)	0.0001	0.0001

Table 5 summarizes the input parameters for heat exchanger design, featuring propane as the hot stream and LNG as the cold stream. Both fluids are in liquid phase. Propane enters the exchanger at −26 °C and exits at −100 °C, while LNG enters at −156 °C and leaves at −136 °C. The operating pressures are 2.14 kg/cm^2 for propane and 56 kg/cm^2 for LNG. For both fluids, the allowable pressure drop is 0.20 kg/cm^2, and the fouling resistance is set at 0.0001 m^2K/W.

Fig. 2 illustrates the schematic of the heat exchanger design simulation, indicating that the LNG flows through the tube section while propane flows through the shell section.

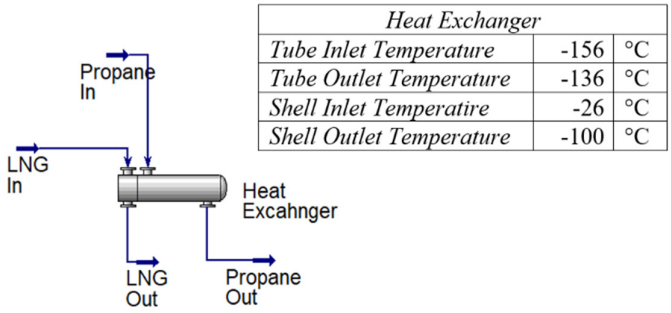

Fig. 2. Schematic of the Heat Exchanger Design Simulation

2.9 Heat Exchanger Configuration Plan

Fig. 3 shows the schematic of the planned heat exchanger installation, based on the modification presented in Fig. 1. It illustrates the revised LNG process flow diagram, where the LNG flow from the storage tank to the ORV is tapped to feed a shell-and-tube heat exchanger, allowing its cold energy to be utilised for multiple cooling applications.

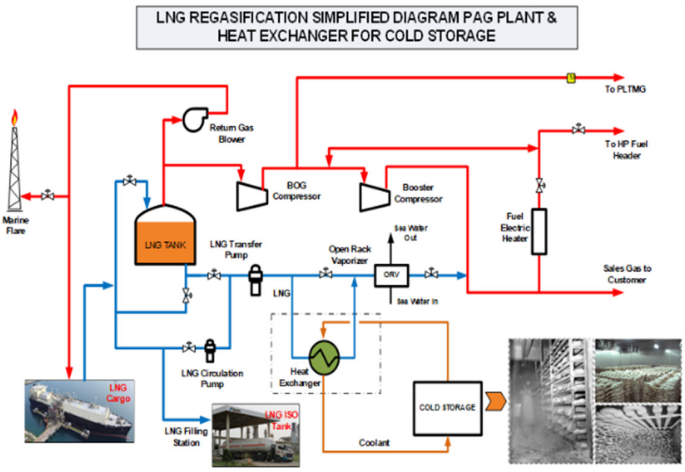

Fig. 3. Schematic of Heat Exchanger Installation Planning

The heat exchanger design is performed using Aspen Exchanger Design and Rating (EDR) software, based on established process and geometric data. In this design, the LNG flow rate for the cold energy extraction process is set at 30 MMSCFD. The design is carried out with variations in the outer diameter of the tube of 13 mm, 16 mm, 19.05 mm, 20 mm, 25 mm, 25.4 mm, 30 mm, and 38 mm. Using this data, the design is carried out through an iteration calculation process by the software until a design is obtained that is by the desired heat exchanger specifications.

3 Result and Discussion

3.1 Heat Exchanger Design Optimisation Analysis

Table 6 summarises the design specifications produced by the Aspen EDR software. The evaluation of the heat exchanger design, as shown in the summarised data, demonstrates a detailed assessment of various configurations that include tube outer diameters (OD), shell diameters, tube lengths, pressure drops, baffle placements, and their corresponding total expenses. From the findings, it is clear that the tube OD has a significant impact on both the thermal efficiency and the cost-effectiveness of the exchanger. Smaller diameters, like 13.00 mm, are linked to lower overall costs (for instance, $23,895 for design No. 1), probably due to decreased material requirements and simpler structural needs. Conversely, as the tube diameter increases, there tends to be an increase in expenses, peaking at $54,100 for a 38.00 mm tube OD (design No. 36), which is likely due to the higher material quantity, larger shell dimensions, and more intricate baffle designs.

Table. 6 Heat exchanger design result data

No	Tube OD (mm)	Shell	Tube Length		Pressure Drop		Baffle		Tube		Total
		Diameter (mm)	Actual (mm)	Required (mm)	Shell (bar)	Tube (bar)	Pitch (mm)	No.	Tube Pass	No	Price (USD)
1	13.00	162.74	2550	2459.10	0.09	0.10	135	16	1	54	23,895
2	13.00	213.54	1500	1498.60	0.10	0.04	70	16	1	100	27,482
3	13.00	213.54	1500	1463.50	0.13	0.15	65	18	2	98	27,007
4	16.00	162.74	3000	2874.80	0.13	0.11	120	22	1	40	27,319
5	16.00	213.54	2100	2043.00	0.11	0.05	80	22	1	69	31,496
6	16.00	213.54	2250	2021.60	0.16	0.26	80	24	2	60	31,059
7	19.05	162.74	3750	3688.60	0.13	0.10	135	24	1	27	27,969
8	19.05	213.54	2550	2549.10	0.10	0.05	100	22	1	47	31,595
9	19.05	213.54	2700	2433.10	0.12	0.21	100	24	2	44	31,649
10	20.00	162.74	4200	4179.60	0.16	0.12	135	28	1	22	28,278
11	20.00	213.54	2850	2781.00	0.18	0.05	80	30	1	40	32,362
12	20.00	213.54	3450	3057.70	0.07	0.27	140	22	2	36	32,929
13	25.00	213.54	3750	3638.80	0.08	0.04	125	26	1	27	33,962
14	25.00	213.54	3600	3447.20	0.12	0.18	110	30	2	26	33,346
15	25.00	266.24	2550	2496.10	0.20	0.03	70	30	1	44	38,016
16	25.00	266.24	2400	2303.90	0.12	0.07	80	24	2	44	36,786
17	25.00	315.93	1800	1725.50	0.13	0.20	65	22	4	60	40,372
18	25.40	213.54	3600	3510.50	0.11	0.04	110	30	1	27	33,935
19	25.40	213.54	3450	3411.80	0.16	0.16	90	34	2	26	33,320
20	25.40	266.24	2850	2842.80	0.10	0.03	90	28	1	40	38,543
21	25.40	266.24	2400	2395.00	0.10	0.07	90	22	2	42	36,427
22	25.40	315.93	1800	1746.60	0.14	0.18	65	22	4	60	40,864
23	30.00	213.54	5250	5139.30	0.18	0.05	110	44	1	15	36,498
24	30.00	213.54	4500	4349.00	0.09	0.16	140	30	2	18	34,830
25	30.00	266.24	3300	3188.60	0.13	0.03	90	32	1	31	40,301
26	30.00	315.93	2550	2539.90	0.15	0.03	65	32	1	44	45,212
27	30.00	315.93	2100	2028.20	0.14	0.18	65	26	4	40	41,378
28	38.00	213.54	6000	6471.90	0.22	0.04	110	50	1	10	37,888
29	38.00	213.54	6000	6326.40	0.15	0.18	125	44	2	10	37,262
30	38.00	266.24	4500	4437.70	0.16	0.03	90	46	1	19	44,345
31	38.00	266.24	4050	3963.00	0.17	0.06	90	40	2	18	41,693
32	38.00	315.93	3600	3561.70	0.15	0.03	75	42	1	27	49,995
33	38.00	315.93	2850	2822.20	0.19	0.04	75	32	2	30	46,227
34	38.00	315.93	3300	2990.50	0.15	0.24	85	34	4	23	46,317
35	38.00	346.05	3000	2963.90	0.15	0.03	80	32	1	37	54,100
36	38.00	346.05	2550	2486.80	0.12	0.03	70	30	2	36	50,820
37	38.00	346.05	2700	2634.60	0.07	0.12	90	26	4	30	49,683

The pressure drop across both the shell and tube sides is critical in assessing the operational efficiency. Most configurations maintain a shell-side pressure drop below 0.20 bar, aligning with common design criteria to minimise pumping costs. Configurations with higher tube lengths and larger shell diameters, such as design No. 29 with a required tube length of 6726.40 mm, tend to exhibit higher pressure drops and total costs. Additionally, the number of tube passes and baffle spacing (pitch) significantly affect heat transfer efficiency and pressure losses. For instance, tighter baffle pitches (e.g., 90 mm in design No. 26) correlate with increased pressure drop but can enhance heat transfer due to increased turbulence.

From an economic standpoint, designs featuring moderate tube diameters (16.00–25.00 mm) provide a good compromise between cost and performance, making them ideal for situations where efficiency and budget limitations are critical. In general, this parametric analysis offers important insights into the compromises associated with shell-and-tube heat exchanger design, aiding in the selection of the best configurations for particular thermal applications.

From the results of the heat exchanger design, it can be identified that the most optimal design, considering the minimum manufacturing costs, is a design with a tube diameter of 13 mm, a tube length of 2550 mm, a shell diameter of 162.74 mm, a baffle pitch of 135 mm, several baffles of 16, several tube passes of 1, and several tubes of 54, which can extract cold energy of 478.5 KW with a manufacturing cost of USD 23,895.

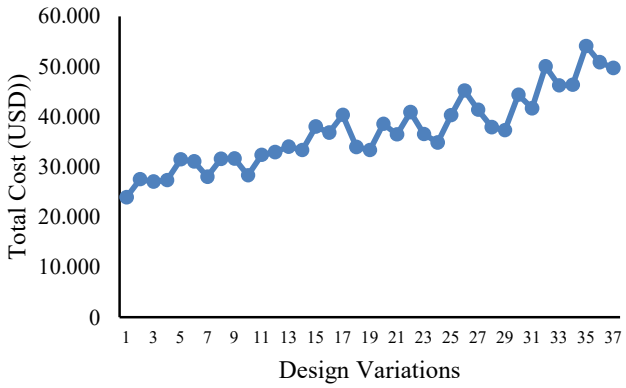

Fig. 4. Cost comparison for 37 heat exchanger design options

Fig. 4 illustrates the variations in overall cost (in USD) across 37 design options. A consistent upward trend is evident, suggesting that more sophisticated designs generally lead to higher costs. The fluctuations observed along the trend likely result from changes in materials, design choices, or efficiency improvements that impact cost. This pattern underscores the importance of carefully balancing design enhancements with their associated expenses to identify the most practical and cost-effective solution.

3.2 Heat Exchanger Specification Data

Fig. 5 presents the heat exchanger specifications for the LNG cold energy extraction process at a flow rate of 30 MMSCFD. The table includes key information such as process conditions, heat transfer parameters, fluid properties, pressure drop, and geometric configurations of the heat exchanger. The heat exchanger design demonstrates efficient thermal and hydraulic performance, delivering a total heat load of 478.5 kW with an effective temperature difference of 80.6°C and a safe pressure drop within allowable limits (0.0821 bar shell side, 0.1063 bar tube side). The use of 54 tubes with a one-pass configuration and single-segmental baffles ensures enhanced heat transfer, supported by turbulent flow regimes (Re > 17,000) and adequate velocity control that avoids vibration or $RhoV^2$ violations. Notably, the geometry data indicates the absence of vibration issues during heat transfer, suggesting that the designed and optimised heat exchanger meets the operational requirements. This implies that the system is structurally stable and well-suited for the cold energy extraction process in LNG regasification, with no indications of vibration-induced instability. Despite fouling contributing 21.26% to thermal resistance, the actual-to-required area ratio (1.36 clean) indicates a sufficient design margin. Overall, the system is well optimised for high-efficiency heat exchange under demanding process conditions.

Fig.s 6 and 7 present the geometric details of the heat exchanger, visualising the results of the design optimisation. The design features a tube diameter of 13 mm, a tube length of 2550 mm, a shell diameter of 162.74 mm, a baffle pitch of 135 mm, 16 baffles, a single tube pass, and 54 tubes. It is designed for cold energy extraction with an LNG flow rate of 30 MMSCFD, enabling a heat transfer of 478.5 kW at a manufacturing cost of USD 23,895. The diagrams validate that the heat exchanger design—with a 162.74 mm shell, 54 tubes (13 mm diameter), single-pass layout, and 135 mm baffle pitch—ensures uniform flow, enhanced heat transfer, and low pressure drop. Operating in a turbulent regime (Re > 17,000) with no vibration issues, the configuration is both thermally efficient and mechanically reliable for LNG cold energy recovery.

Size	0.1627	X	2.55	m	Type	BEM	Hor		Connected in	1	parallel	1	series		
Surf/Unit (gross/eff/finned)			5.6	/ 5.5	/			m²	Shells/unit	1					
Surf/Shell (gross/eff/finned)			5.6	/ 5.5	/			m²							
Design (Sizing)						PERFORMANCE OF ONE UNIT									
			Shell Side			Tube Side			Heat Transfer Parameters						
Process Data			In	Out		In	Out		Total heat load			kW		478.5	
Total flow		kg/h		10756			25130		Eff. MTD/ 1 pass MTD			°C	80.61	/	80.6
Vapor		kg/h	0	0		0	0		Actual/Reqd area ratio - fouled/clean				1.04	/	1.36
Liquid		kg/h	10756	10756		25130	25130								
Noncondensable		kg/h		0			0		Coef./Resist.		W/(m²-K)	m²-K/W		%	
Cond./Evap.		kg/h		0			0		Overall fouled		1123.2	0.00089			
Temperature		°C	-26	-100		-156	-136		Overall clean		1468.6	0.00068			
Dew / Bubble point		°C	-23.89	-23.89					Tube side film		5283	0.00019		21.26	
Quality			0	0		0	0		Tube side fouling		9140.3	0.00011		12.29	
Pressure (abs)		bar	2.1	2.01295		54.91724	54.81406		Tube wall		22215.7	5E-05		5.06	
DeltaP allow/cal		bar	0.2	0.08705		0.2	0.10319		Outside fouling		10000	0.0001		11.23	
Velocity		m/s	1.01	0.88		2.73	2.95		Outside film		2238.9	0.00045		50.16	
Liquid Properties									Shell Side Pressure Drop				bar	%	
Density		kg/m³	562.59	644.24		426.37	395.02		Inlet nozzle				0.00481	5.52	
Viscosity		mPa-s	0.1669	0.423		0.1101	0.0744		InletspaceXflow				0.00404	4.63	
Specific heat		kJ/(kg-K)	2.319	2.064		3.335	3.541		Baffle Xflow				0.0425	48.69	
Therm. cond.		W/(m-K)	0.1203	0.1608		0.1804	0.1498		Baffle window				0.02914	33.39	
Surface tension		N/m							OutletspaceXflow				0.00384	4.4	
Molecular weight			44.1	44.1		16.64	16.64		Outlet nozzle				0.00294	3.37	
Vapor Properties									Intermediate nozzles						
Density		kg/m³							Tube Side Pressure Drop				bar	%	
Viscosity		mPa-s							Inlet nozzle				0.01289	12.81	
Specific heat		kJ/(kg-K)							Entering tubes				0.00753	7.48	
Therm. cond.		W/(m-K)							Inside tubes				0.05616	55.79	
Molecular weight									Exiting tubes				0.01006	10	
Two-Phase Properties									Outlet nozzle				0.01401	13.92	
Latent heat		kJ/kg							Intermediate nozzles						
Heat Transfer Parameters									Velocity / Rho*V2			m/s		kg/(m-s²)	
Reynolds No. vapor									Shell nozzle inlet			1.11		697	
Reynolds No. liquid			44175.62	17422.32		125765	186131		Shell bundle Xflow		1.01	0.88			
Prandtl No. vapor									Shell baffle window		0.95	0.83			
Prandtl No. liquid			3.22	5.43		2.04	1.76		Shell nozzle outlet			0.97		609	
Heat Load				kW			kW		Shell nozzle interm						
Vapor only				0			0					m/s		kg/(m-s²)	
2-Phase vapor				0			0		Tube nozzle inlet			2.57		2809	
Latent heat				0			0		Tubes		2.73	2.95			
2-Phase liquid				0			0		Tube nozzle outlet			3.71		5423	
Liquid only				-478.5			478.5		Tube nozzle interm						
Tubes						Baffles			Nozzles: (No./OD)				Shell Side		Tube Side
Type					Plain	Type	Single segmental								
ID/OD		mm	11.88	/	13	Number		16	Inlet	mm	1	/ 88.9	1	/	101.6
Length act/eff		mm	2550	/	2485	Cut(%d)		41.35	Outlet		1	/ 88.9	1	/	88.9
Tube passes			1			Cut orientation		H	Intermediate			/		/	
Tube No.			54			Spacing: c/c	mm	135	Impingement protection			None			
Tube pattern			30			Spacing at inlet	mm	229.98							
Tube pitch		mm	16.25			Spacing at outlet	mm	229.98							
Insert					None										
Vibration problem				No	/ No				RhoV2 violation						No

Fig. 5. Heat exchanger specification data

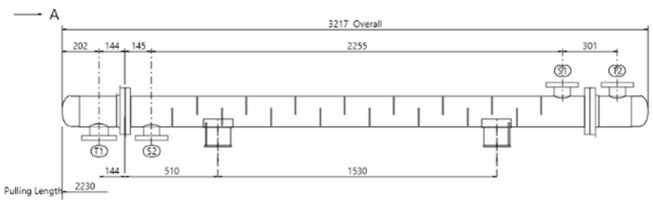

Fig. 6. Heat exchanger setting plan

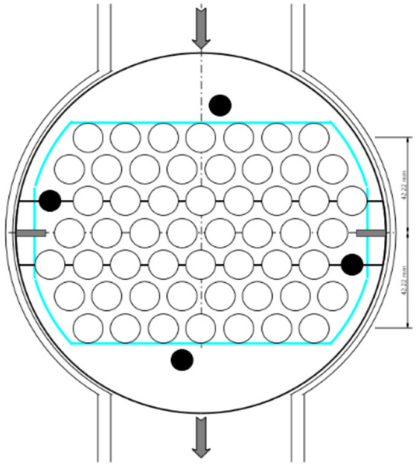

Fig. 7. Heat exchanger tubesheet layout

4 Conclusion

Based on the design optimisation results, it can be concluded that the most optimal shell-and-tube heat exchanger design for cold energy extraction in the LNG regasification process at PT Perta Arun Gas is a configuration with a tube diameter of 13 mm, a tube length of 2550 mm, a shell diameter of 162.74 mm, a baffle pitch of 135 mm, 16 baffles, a single tube pass, and 54 tubes. This design is capable of extracting 478.5 kW of cold energy with a manufacturing cost of USD 23,895. Beyond this specific case, the optimised design holds significant potential for various industrial applications, such as data centre cooling, cold storage facilities, and district cooling systems. Future research should focus on scaling the heat exchanger for different LNG flow rates, evaluating its performance under varying operating conditions, and integrating it with other energy recovery systems. Moreover, implementing such cold energy recovery technologies contributes to improved energy efficiency and helps reduce thermal emissions to the environment, supporting broader sustainability goals in the LNG sector.

Acknowledgement

The authors would like to express their sincere gratitude to P.T. Perta Arun Gas for generously providing access to the LNG regasification process data.

References

[1] J. Pan, R. Li, T. Lv, and G. Wu, "Thermal performance analysis of SuperORV heat transfer tube at supercritical pressure," *J. Nat. Gas Sci. Eng.*, vol. 29, pp. 488–496, 2016, doi: https://doi.org/10.1016/j.jngse.2016.01.030.

[2] H. Cheng, Y. Ju, and Y. Fu, "Thermal performance calculation with heat transfer correlations and numerical simulation analysis for typical LNG open rack vaporizer," *Appl. Therm. Eng.*, vol. 149, pp. 1069–1079, 2019, doi: https://doi.org/10.1016/j.applthermaleng.2018.11.044.

[3] S. Cao, T. Luan, P. Zuo, X. Si, P. Xie, and Y. Guo, "Simulation and Economic Benefit Analysis of Carburetor Combined Transport in Winter at a Liquefied Natural Gas Receiving Station," 2025. doi: 10.3390/en18020276.

[4] C. Qi, W. Wang, B. Wang, Y. Kuang, and J. Xu, "Performance analysis of submerged combustion vaporizer," *J. Nat. Gas Sci. Eng.*, vol. 31, pp. 313–319, 2016, doi: https://doi.org/10.1016/j.jngse.2016.03.003.

[5] K. Huang, X. Zhou, C. Huang, L. Wang, D. Li, and J. Zhao, "Heat Transfer Analysis and Operation Optimization of an Intermediate Fluid Vaporizer," 2023. doi: 10.3390/en16031383.

[6] L. N. Guo, B. L. An, L. B. Chen, J. X. Chen, J. J. Wang, and Y. Zhou, "Progress of liquefied natural gas cold energy utilization," *IOP Conf. Ser. Mater. Sci. Eng.*, vol. 502, no. 1, p. 12148, 2019, doi: 10.1088/1757-899X/502/1/012148.

[7] J. Pospíšil, P. Charvát, O. Arsenyeva, L. Klimeš, M. Špiláček, and J. J. Klemeš, "Energy demand of liquefaction and regasification of natural gas and the potential of LNG for operative thermal energy storage," *Renew. Sustain. Energy Rev.*, vol. 99, pp. 1–15, 2019, doi: https://doi.org/10.1016/j.rser.2018.09.027.

[8] M. Zonfrilli, M. Facchino, R. Serinelli, M. Chesti, M. De Falco, and M. Capocelli, "Thermodynamic analysis of cold energy recovery from LNG regasification," *J. Clean. Prod.*, vol. 420, p. 138443, 2023, doi: https://doi.org/10.1016/j.jclepro.2023.138443.

[9] A. Soh, Z. Huang, Y. Shao, M. R. Islam, and K. J. Chua, "On the study of a thermal system for continuous cold energy harvesting and supply from LNG regasification," *Energy*, vol. 275, p. 127387, 2023, doi: https://doi.org/10.1016/j.energy.2023.127387.

[10] T. He, J. Ma, H. Ma, and T. Jin, "Chapter 14 - Exploiting cold energy associated with LNG regasification processes," in *The Fundamentals and Sustainable Advances in Natural Gas Science and Engineering*, vol. 3, D. A. Wood and J. B. T.-S. L. N. G. Cai, Eds., Elsevier, 2024, pp. 399–424. doi: https://doi.org/10.1016/B978-0-443-13420-3.00011-1.

[11] S. E. Sofyan *et al.*, "The potential of cold energy extraction from a power plant regasification terminal for cold storage application," *IOP Conf. Ser. Mater. Sci. Eng.*, vol. 1082, no. 1, p. 12007, 2021, doi: 10.1088/1757-899X/1082/1/012007.

[12] F. Yehia *et al.*, "Integration of the single-effect mixed

refrigerant cycle with liquified air energy storage and cold energy of LNG regasification: Energy, exergy, and efficiency prospectives," *Energy*, vol. 306, p. 132567, 2024, doi: https://doi.org/10.1016/j.energy.2024.132567.

[13] M. H. Noor Akashah, N. E. Mohammad Rozali, S. Mahadzir, and P. Y. Liew, "Utilization of Cold Energy from LNG Regasification Process: A Review of Current Trends," 2023. doi: 10.3390/pr11020517.

[14] W. Gazda, "Application possibilities of the strategies of the air blast–cryogenic cooling process," *Energy*, vol. 62, pp. 113–119, 2013, doi: https://doi.org/10.1016/j.energy.2013.06.054.

[15] J. Lim, Y. Kim, H. Cho, J. Lee, and J. Kim, "Novel process design for waste energy recovery of LNG power plants for CO2 capture and storage," *Energy Convers. Manag.*, vol. 277, p. 116587, 2023, doi: https://doi.org/10.1016/j.enconman.2022.116587.

[16] S. Yadav, S. Seethamraju, and R. Banerjee, "Cold energy recovery from liquefied natural gas regasification process for data centre cooling and power generation," *Energy*, vol. 283, p. 128481, 2023, doi: https://doi.org/10.1016/j.energy.2023.128481.

[17] X. Zheng *et al.*, "Performance analysis and multi-objective optimization for an integrated air separation, power generation, refrigeration and ice thermal storage system based on the LNG cold energy utilization," *Int. J. Refrig.*, vol. 168, pp. 521–536, 2024, doi: https://doi.org/10.1016/j.ijrefrig.2024.07.008.

[18] D. Cai, Y. Zhao, Y. Wang, H. Liu, Y. Liang, and D. Hu, "Comparative analysis: Exergetic and economic assessment of LNG cold energy power generation systems with different cold utilization methods," *Therm. Sci. Eng. Prog.*, vol. 54, p. 102844, 2024, doi: https://doi.org/10.1016/j.tsep.2024.102844.

[19] X. Wang, M. Zhu, W. Han, Z. Wu, and S. Chen, "Cold energy utilization analysis of cryogenic dual-energy heavy-duty trucks coupled LH2/LNG cooled shield," *Int. J. Hydrogen Energy*, vol. 71, pp. 387–399, 2024, doi: https://doi.org/10.1016/j.ijhydene.2024.05.135.

[20] A. Franco and C. Giovannini, "Optimal design of direct expansion systems for electricity production by LNG cold energy recovery," *Energy*, vol. 280, p. 128173, 2023, doi: https://doi.org/10.1016/j.energy.2023.128173.

[21] W. Wu, S. Xie, J. Tan, and T. Ouyang, "An integrated design of LNG cold energy recovery for supply demand balance using energy storage devices," *Renew. Energy*, vol. 183, pp. 830–848, 2022, doi: https://doi.org/10.1016/j.renene.2021.11.066.